

Analyzing powers for ${}^9\text{Be}({}^6\bar{\text{Li}}, {}^6\text{He}){}^9\text{B}$

E. L. Reber, K. W. Kemper, P. L. Kerr, A. J. Mendez, E. G. Myers,
and B. G. Schmidt

Department of Physics, Florida State University, Tallahassee, Florida 32306

N. M. Clarke

School of Physics and Space Research, University of Birmingham, Birmingham, B15 2TT, United Kingdom

(Received 5 November 1992)

Vector and tensor analyzing powers (iT_{11} , T_{20} , T_{20} , and T_{22}) for the ${}^9\text{Be}({}^6\bar{\text{Li}}, {}^6\text{He}){}^9\text{B}$ reaction are presented for a ${}^6\bar{\text{Li}}$ bombarding energy of 32 MeV over the angular range from 14° to 80° c.m. A one-step reaction calculation is consistent with the angular distribution and vector analyzing power iT_{11} for the ground-state transition but does not describe the tensor analyzing power T_{20} . Coupled channels calculations that include inelastic coupling in the entrance and exit channels do not reproduce either the vector or tensor analyzing powers. Sequential transfer calculations via $({}^6\text{Li}, {}^7\text{Li})({}^7\text{Li}, {}^6\text{He})$ do not reproduce the ground-state angular distribution but do reproduce the analyzing powers. The analyzing power data to the ${}^9\text{B}(\frac{5}{2}^-, 2.36 \text{ MeV state})$ are well reproduced by the coupled channels calculation although the cross section is under predicted by a factor of 3.

PACS number(s): 24.70.+s, 25.70.Kk

The possibility that the $({}^6\text{Li}, {}^6\text{He})$ reaction might provide new information on Gamow-Teller (GT) strength in nuclei has been discussed for about 20 years [1, 2]. The fact that the forbidden $0^+ \rightarrow 0^+$ transition at 32 MeV bombarding energy in the ${}^{26}\text{Mg} \rightarrow {}^{26}\text{Al}$ reaction [3] has a cross section of 10% of that of the allowed $0^+ \rightarrow 1^+$ transition suggests that multistep reaction processes might not be a large contamination to the assumed one-step charge exchange process. However, recent studies [4] of $({}^6\text{Li}, {}^6\text{He})$ have emphasized the need to go to energies above 25 MeV per nucleon before the $({}^6\text{Li}, {}^6\text{He})$ reaction becomes one step and hence can be used to extract reliable GT strengths. Calculations [5, 6] that use the same magnitude forces as those describing the 25 MeV per nucleon data are able to describe charge exchange data at energies as low as 5 MeV per nucleon. To date, the only observables used in the study of these charge exchange reactions are cross sections, ratios of cross sections, and angular distributions. It is important to investigate the ability of other reaction observables to discriminate between reaction modes.

The reliability and intensity of polarized Li ion sources [7, 8] has become sufficiently good to allow analyzing power measurements to be made for the $({}^6\text{Li}, {}^6\text{He})$ reaction. The present work reports the first measurements of vector and tensor analyzing powers for the ${}^9\text{Be}({}^6\bar{\text{Li}}, {}^6\text{He}){}^9\text{B}$ reaction at the ${}^6\bar{\text{Li}}$ bombarding energy of 32 MeV. This reaction was chosen for this initial study because the charge exchange cross sections [5] are large and a microscopic analysis of the reaction using the M3Y interaction described both the magnitude and shape of the angular distribution data. In the present work, the results of these microscopic calculations as well as results of a coupled channels and a sequential transfer calculation are compared to the analyzing power data.

The Florida State University optically pumped polarized Li ion source and FN Tandem Van de Graaff were used to supply a beam of 32 MeV polarized ${}^6\text{Li}^{3+}$ ions that bombarded a self-supporting ${}^9\text{Be}$ target of thickness $200 \mu\text{g}/\text{cm}^2$. The experiment used four $\Delta E - E$ telescopes to identify the reaction products. The detector resolution was 150 keV. Two telescopes were arranged symmetrically on each side of the beam axis. The polarization of the ${}^6\text{Li}$ beam was monitored using a helium filled polarimeter that follows the main scattering chamber. The beam energy was decreased to 15.5 MeV at the center of the polarimeter target volume by passing it through Al foils before it enters the polarimeter. Detectors were placed at $\theta_{\text{lab}} = \pm 15^\circ$ to monitor the reaction ${}^4\text{He}({}^6\bar{\text{Li}}, \alpha){}^6\text{Li}$. This reaction was used because of its large cross sections [9] and vector analyzing powers [10] at 15.5 MeV. Recent work [8] has also shown that at this angle, the tensor analyzing powers are large enough to serve as a beam polarization monitor.

The three magnetic substates of the ${}^6\bar{\text{Li}}$ beam are $m_I = +1(N_+)$, $m_I = 0(N_0)$, and $m_I = -1(N_-)$, and when the beam was unpolarized it was defined as being in the off state. The data were taken in cycles with each cycle consisting of accumulating data in the off, N_+ , N_0 , and N_- states. The states were changed every 2 min.

The typical beam current on target was 30–50 electrons nA. The vector beam polarization [8] was determined to be $t_{10} = 1.02 \pm 0.05$ and the tensor beam polarization was $t_{20} = -0.92 \pm 0.05$. The Madison convention [11] is used in this work for description of polarization observables. When, however, quantities relating to a frame in which the spin quantization axis is normal to the scattering plane, the “transverse” frame is employed, they are denoted by a left superscript T .

The vector and tensor analyzing powers (VAP and

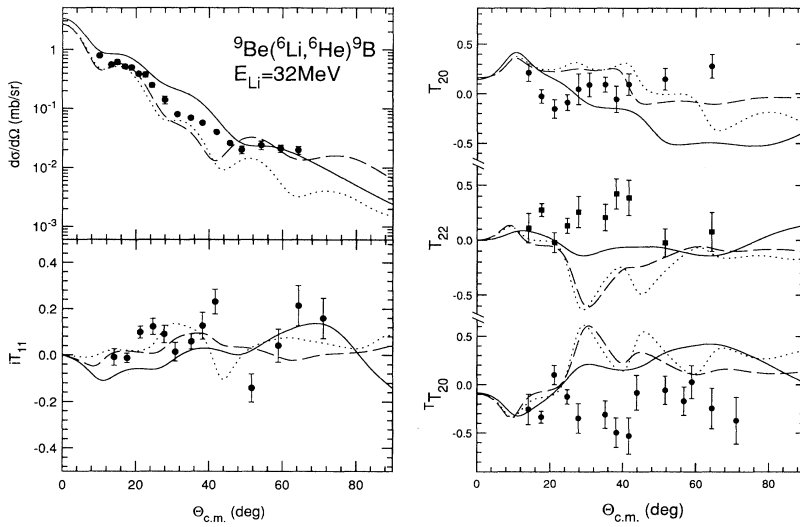


FIG. 1. Differential cross sections and analyzing powers for the reaction ${}^9\text{Be}({}^6\text{Li}, {}^6\text{He}){}^9\text{B}$ at $E_{\text{Li}} = 32$ MeV. The dashed curves are the result of DWBA calculations using the new shell model spectroscopic amplitudes. The dotted curves show the sequential contributions via the $\frac{5}{2}^-$ state in ${}^9\text{Be}$. The solid curves are the full CCBA calculations for the reaction ${}^9\text{Be}({}^6\text{Li}, {}^6\text{He}){}^9\text{B}$ which include all the direct and sequential contributions from inelastic coupling in both ${}^9\text{Be}$ and ${}^9\text{B}$. The coupling scheme is shown in Figure 3.

TAP) were both measured in the angular range from 14° to 80° c.m. The size of the error bars in the figures show the statistical uncertainty in the analyzing powers. The VAP were measured with the polarization axis normal to the scattering plane and determined by

$$iT_{11} = \frac{L - R}{2\sqrt{2} t_{10}}, \quad (1)$$

where $L = L_{\text{pol}}/L_{\text{unpol}}$ and $R = R_{\text{pol}}/R_{\text{unpol}}$. L_{pol} (R_{pol}) and L_{unpol} (R_{unpol}) represent the number of particles accumulated in the detector to the left (right) of the beam when the ${}^6\text{Li}$ was polarized and unpolarized, respectively. The beam contains vector and tensor components in all three spin states N_+ , N_0 , and N_- so that using L and R symmetrically placed detectors allow the two analyzing powers iT_{11} and T_{20} to be determined for each spin state. The VAP were also computed for each left and right detector separately by using the N_+ and N_- states to make certain that no change in efficiency of the de-

tector pair occurred during the runs. The TAP were determined from the results

$$T_{20} = \frac{L + R - 2}{2 t_{20}}, \quad (2)$$

with the polarization axis aligned normal to the scattering plane, and

$$T_{20} = \frac{L + R - 2}{2 t_{20}} \quad (3)$$

with the polarization axis parallel to the beam axis. From the measured quantities T_{20} and T_{22} was deduced using the relation

$$T_{22} = -\sqrt{\frac{1}{6}} T_{20} - \sqrt{\frac{2}{3}} T_{20}. \quad (4)$$

Distorted wave Born approximation (DWBA) calculations were made with the code CHUCK [12] using the optical parameters of Cook and Kemper [5] and form

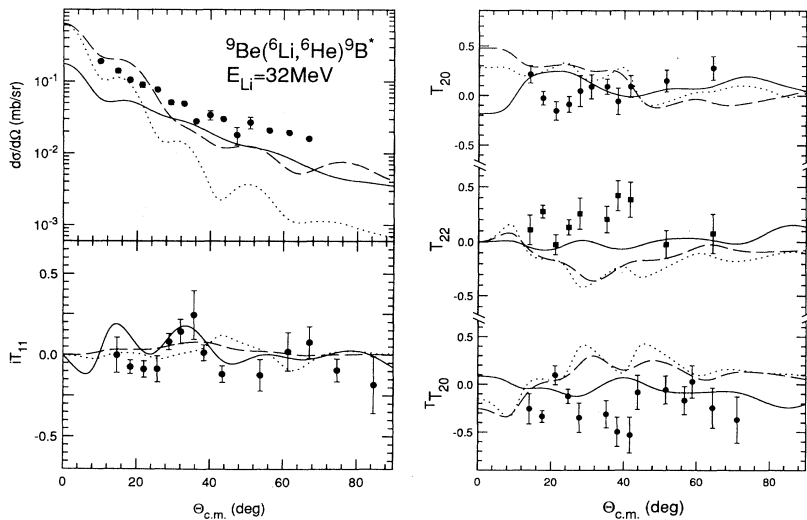


FIG. 2. Differential cross sections and analyzing powers for the reaction ${}^9\text{Be}({}^6\text{Li}, {}^6\text{He}){}^9\text{B}^*$ at $E_{\text{Li}} = 32$ MeV. The dashed curves are the result of DWBA calculations using the new shell model spectroscopic amplitudes. The dotted curves show the sequential contributions via the $\frac{5}{2}^-$ state in ${}^9\text{Be}$. The solid curves are the full CCBA calculations for the reaction ${}^9\text{Be}({}^6\text{Li}, {}^6\text{He}){}^9\text{B}$ with the coupling scheme as shown in Figure 3.

TABLE I. Shell model spectroscopic amplitudes $S_{TM_T}^J(j_f j_i)$ for the ${}^9\text{Be}({}^6\text{Li}, {}^6\text{He}){}^9\text{B}$ reaction.

Final state	$p_{\frac{1}{2}}$	$p_{\frac{3}{2}}$	$p_{\frac{1}{2}}^{-1}$	$p_{\frac{3}{2}}^{-1}$
Initial state	$p_{\frac{1}{2}}^{-1}$	$p_{\frac{3}{2}}^{-1}$	$p_{\frac{1}{2}}$	$p_{\frac{3}{2}}$
${}^9\text{Be}(\text{g.s.}) \rightarrow {}^9\text{B}(\text{g.s.})$				
$J=0$	0.0139	0.0	0.0	1.310
1	-0.0869	-0.1381	-0.0565	0.8264
2	0.0	0.1905	-0.059	0.1753
3	0.0	0.0	0.0	0.9698
${}^9\text{Be}(\frac{5}{2}^-, 2.43 \text{ MeV}) \rightarrow {}^9\text{B}(\text{g.s.})$				
$J=1$	-0.0042	-0.1521	-0.166	-0.9753
2	0.0	-0.4053	-0.039	-0.8618
3	0.0	0.0	0.0	0.5362

factors for the direct charge exchange reaction calculated with the code CHEX2 [13]. In this code, the bound state wave functions were calculated by the separation energy procedure in Woods-Saxon potential wells with geometry parameters of $r_0 = 1.25$ fm and $a = 0.65$ fm. The spectroscopic amplitudes for ${}^6\text{Li} \rightarrow {}^6\text{He}$, ${}^9\text{Be} \rightarrow {}^9\text{B}_{\text{g.s.}}$, and ${}^9\text{Be} \rightarrow {}^9\text{B}_{\frac{5}{2}^-}$ were taken from Ref. [5], and the form factors for all L , S , J transfers were calculated according to the formalism of Cook *et al.* [14], using both the central and tensor parts of the $T = 1$, M3Y interaction. These calculations gave very good agreement with those of Ref. [5]; the shape and magnitude of the differential cross sections for the ${}^9\text{B}_{\text{g.s.}}$ are well predicted, as shown in Fig. 1. For the ${}^9\text{B}_{\frac{5}{2}^-}$ transition, the magnitude is underpredicted by a factor of 3, but, as shown in Fig. 2, the shape is in reasonable agreement with the data. A source of this error might be due to the fact that the shell model calculations for ${}^9\text{B}$ were carried out in a spherical basis.

The coupled channels (CC) analyses of Ref. [5] showed that a much better description of the elastic and inelastic scattering angular distribution of ${}^6\text{Li}$ from ${}^9\text{Be}$ could be obtained using a deformation length of $\delta_2 = 1.9$ fm, consistent with the $B(E2)$ of $45.7 e^2 \text{ fm}^4$ for the $\frac{3}{2}^-$ to $\frac{5}{2}^-$ inelastic transition in ${}^9\text{Be}$. In addition, extensive analyses [15] have shown that virtual excitation of ${}^6\text{Li}$ during the scattering process gives rise to the observed elastic vector analyzing power, suggesting that this coupling could be important in the charge exchange process. In order

to include the effects of this strong inelastic coupling in both the ${}^6\text{Li} + {}^9\text{Be}$ and ${}^6\text{He} + {}^9\text{B}$ channels, a new set of spectroscopic amplitudes were calculated for the direct charge exchange from both the $\frac{3}{2}^-$ and $\frac{5}{2}^-$ states in ${}^9\text{Be}$ to both the mirror states in ${}^9\text{B}$. The one-body-transition densities were calculated using the OXBASH code [16] with the (6-16) TBME Cohen-Kurath p -shell interaction, then converted to spectroscopic amplitudes [17]. The amplitudes are given in Tables I and II. For each transition, there are five form factors with transferred L , S , and J of 011, 211, 212, 213, and 413; the form factors with L , S , J of 011, 213, and 413 are generally the largest. DWBA calculations using the new form factors gave similar results for the differential cross sections to the calculations of Ref. [5].

Coupled channels (CC) calculations were made which coupled the $\frac{3}{2}^-$ and $\frac{5}{2}^-$ states in ${}^9\text{Be}$, including both the direct charge exchange to the $\frac{3}{2}^-$ and $\frac{5}{2}^-$ states in ${}^9\text{B}$, as well as the sequential contributions via the $\frac{5}{2}^-$ state in ${}^9\text{Be}$. The CC parameters of Ref. [5] were used, together with a deformation length $\delta_2 = 1.9$ fm for both real and imaginary potentials. Figure 3 shows the couplings used in the calculation. Figures 1 and 2 show the sequential contributions to the differential cross sections for both states in ${}^9\text{B}$. For the ${}^9\text{B}(\text{g.s.})$ state the sequential contribution is small, but it is larger for the ${}^9\text{B}(\frac{5}{2}^-)$ state. The predicted analyzing powers (Figs. 1 and 2) show a

TABLE II. Shell model spectroscopic amplitudes $S_{TM_T}^J(j_f j_i)$ for the ${}^9\text{Be}({}^6\text{Li}, {}^6\text{He}){}^9\text{B}^*$ reaction to the ${}^9\text{B}(\frac{5}{2}^-)$ excited state at 2.36 MeV.

Final state	$p_{\frac{1}{2}}$	$p_{\frac{3}{2}}$	$p_{\frac{1}{2}}^{-1}$	$p_{\frac{3}{2}}^{-1}$
Initial state	$p_{\frac{1}{2}}^{-1}$	$p_{\frac{3}{2}}^{-1}$	$p_{\frac{1}{2}}$	$p_{\frac{3}{2}}$
${}^9\text{Be}(\text{g.s.}) \rightarrow {}^9\text{B}(\frac{5}{2}^-, 2.36 \text{ MeV})$				
$J=1$	-0.0439	-0.1919	-0.156	-0.376
2	0.0	0.1884	-0.4116	-0.4928
3	0.0	0.0	0.0	0.330
${}^9\text{Be}(\frac{5}{2}^-, 2.43 \text{ MeV}) \rightarrow {}^9\text{B}(\frac{5}{2}^-, 2.36 \text{ MeV})$				
$J=0$	0.355	0.0	0.0	0.8422
1	0.255	-0.3034	0.3069	0.4936
2	0.0	0.3196	0.4176	-0.0193
3	0.0	0.0	0.0	0.8623

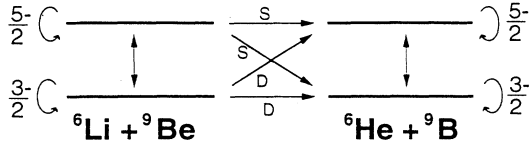


FIG. 3. Full CCBA calculation coupling scheme for the reaction ${}^9\text{Be}({}^6\text{Li}, {}^6\text{He}){}^9\text{B}$.

greater amount of structure than the DWBA predictions.

In the full CCBA calculation, all the direct and sequential contributions were included in addition to the coupling between the ${}^9\text{B}(\text{g.s.})$ and ${}^9\text{B}(\frac{5}{2}^-)$ states, using identical CC parameters and deformation lengths for ${}^6\text{He} + {}^9\text{B}$ as for ${}^6\text{Li} + {}^9\text{Be}$. The results of these calculations are shown in Figs. 1 and 2. The differential cross section for the ${}^9\text{B}(\text{g.s.})$ state is slightly overpredicted when all the couplings are included, while the ${}^9\text{B}(\frac{5}{2}^-)$ state is still underpredicted, but less so than for the DWBA calculations (Figs. 1 and 2). The VAP for the ${}^9\text{B}(\text{g.s.})$ transition are better described by the DWBA calculations. Neither calculation yields a satisfactory description of the TAP, especially ${}^7T_{20}$, which is negative over the whole angular range, whereas the calculations are positive except at the smallest angles. For the ${}^9\text{B}(\frac{5}{2}^-)$ state, the CCBA calculations give a reasonable description of all of the analyzing powers, while the DWBA calculations do not. Calculations were also performed which coupled the ${}^6\text{Li}(3^+)$ state in the entrance channel, but this coupling has only a small effect upon the differential cross sections and analyzing powers in the ${}^6\text{He} + {}^9\text{B}$ channels, and do not improve the description of the data.

Further calculations have been made using the FRESKO code [18] to examine the sequential contribution from the neutron pickup-proton stripping process ${}^9\text{Be}({}^6\text{Li}, {}^7\text{Li}(\text{g.s.} + \frac{1}{2}^-)){}^8\text{Be}(\text{g.s.})({}^7\text{Li}(\text{g.s.} + \frac{1}{2}^-), {}^6\text{He}){}^9\text{B}(\text{g.s.})$. Early discussions [19] of

the $({}^6\text{Li}, {}^6\text{He})$ reaction had suggested that this reaction route is able to explain the magnitude of spin-forbidden $({}^6\text{Li}, {}^6\text{He})$ transitions and further might yield a substantial portion of the allowed differential cross sections. The predicted differential cross section to the ${}^9\text{B}(\text{g.s.})$ state and the predicted analyzing powers are shown in Fig. 4. The contribution to the ${}^9\text{B}(\text{g.s.})$ differential cross section is about a factor of 3 smaller than that predicted by the direct reaction, except at larger angles. The description of the analyzing powers is better, especially for ${}^7T_{20}$, than for either the direct or the CCBA calculations. These predictions should be treated only as an estimate of this sequential contribution; the optical parameters for the ${}^7\text{Li} + {}^8\text{Be}$ channel cannot be known, and there may be effects from the coupling of higher excited states in both ${}^7\text{Li}$ and ${}^8\text{Be}$. It should be noted that the sequential contribution via the ${}^7\text{Li}(\text{g.s.} + \frac{1}{2}^-) + {}^8\text{Be}(0^+)$ channel can affect only the analyzing powers for the ${}^9\text{B}(\text{g.s.})$ state since it cannot populate the ${}^9\text{B}(\frac{5}{2}^-)$ state in first order, because the amplitude for an $f_{\frac{5}{2}}$ proton in ${}^9\text{B}$ must be very small. Any contribution to the ${}^9\text{B}(\frac{5}{2}^-)$ state must therefore arise from inelastic coupling via the ground-state contribution, or via a $p_{\frac{3}{2}}$ or $p_{\frac{1}{2}}$ transfer following excitation of the 2^+ state in ${}^8\text{Be}$, which is unbound. This may explain the relatively good description by CCBA to the ${}^9\text{B}(\frac{5}{2}^-)$ state, where inelastic processes play a dominant role, and the poorer fit to the ${}^9\text{B}(\text{g.s.})$ state, where sequential transfer may be significant.

In summary, the first analyzing powers for the $({}^6\text{Li}, {}^6\text{He})$ reaction are reported. A new set of spectroscopic amplitudes has been derived from shell model calculations for charge exchange from the ${}^9\text{Be}$ g.s. and $\frac{5}{2}^-$ states to the mirror states in ${}^9\text{B}$. CCBA calculations show that the sequential contributions via the first excited state of ${}^9\text{Be}(\frac{5}{2}^-)$ are smaller than the direct transitions from the ${}^9\text{Be}(\text{g.s.})$ state. Full CCBA calculations

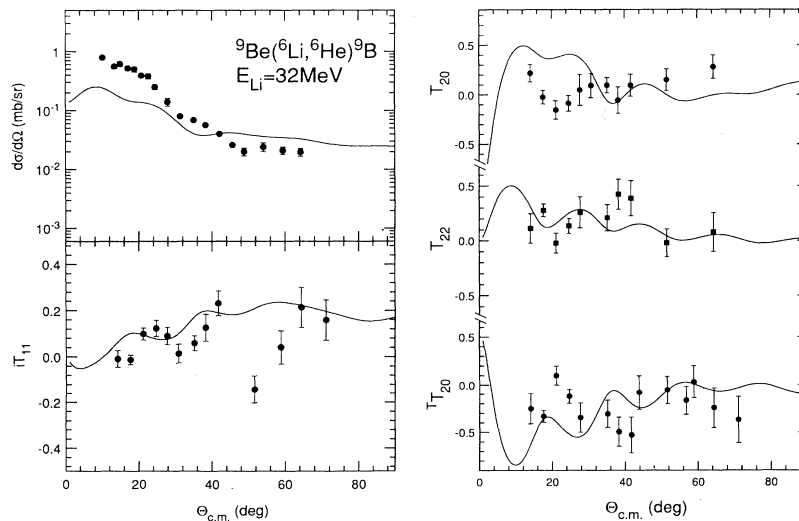


FIG. 4. Differential cross sections and analyzing powers for the reaction ${}^9\text{Be}({}^6\text{Li}, {}^6\text{He}){}^9\text{B}$ at $E_{\text{Li}} = 32$ MeV. The curves are FRESKO calculations which examine the sequential contribution from the neutron pickup-proton stripping process ${}^9\text{Be}({}^6\text{Li}, {}^7\text{Li}(\text{g.s.} + \frac{1}{2}^-)){}^8\text{Be}(\text{g.s.})({}^7\text{Li}(\text{g.s.} + \frac{1}{2}^-), {}^6\text{He}){}^9\text{B}(\text{g.s.})$.

which also couple the ${}^9\text{B}$ (g.s.) and excited state ($\frac{5}{2}^-$) slightly overpredict (underpredict) the differential cross sections for the ${}^9\text{B}$ (g.s.) state ($\frac{5}{2}^-$ state) and fail to reproduce the ${}^9\text{B}$ (g.s.) analyzing powers, although those for the ${}^9\text{B}$ excited state ($\frac{5}{2}^-$) are quite well described. Exact finite range CCBA calculations of the sequential contribution via the ${}^7\text{Li}$ (g.s. and $\frac{1}{2}^-$) + ${}^8\text{Be}$ (g.s.) channels indicate that this process is much smaller than the direct charge exchange reaction except at larger angles. The direct one-step process yields the best description of the ground-state angular distribution and vector ana-

lyzing power. The calculations of the sequential transfer (${}^6\text{Li}, {}^7\text{Li}$)(${}^7\text{Li}, {}^6\text{He}$) suggest that the tensor analyzing powers are sensitive to this reaction contribution and might be useful for determining the magnitude of its contribution to the reaction process.

The authors would like to express their gratitude to Dr. C. N. Pinder for his calculations of the one-body transition densities of this work. This work was supported in part by the National Science Foundation and the State of Florida.

-
- [1] V. I. Chuev, V. V. Davydov, V. I. Manko, B. G. Novatsky, S. B. Sakuta, and D. N. Stepanov, *Phys. Lett.* **31B**, 624 (1970); H. H. Duhm, N. Ueta, W. Heinecke, H. Hafner, H. Homeyer, and P. D. Kunz, *ibid.* **38B**, 306 (1972); W. R. Wharton and P. T. Debevec, *ibid.* **51B**, 451 (1974).
- [2] C. Gaarde and T. Kammuri, *Nucl. Phys.* **A221**, 238 (1974).
- [3] H. H. Duhm, H. Hafner, R. Renfordt, M. Goldschmidt, O. Dragoun, and K. -I. Kubo, *Phys. Lett.* **48B**, 1 (1974).
- [4] J. S. Winfield, N. Anantaraman, S. M. Austin, Z. Chen, A. Galonsky, J. van der Plicht, H. -L. Wu, C. C. Chang, and G. Ciangaru, *Phys. Rev. C* **35**, 1734 (1987); N. Anantaraman, J. S. Winfield, S. M. Austin, J. A. Carr, C. Djalali, A. Gillibert, W. Mittag, J. A. Nolen, Jr., and Z. W. Long, *Phys. Rev. C* **44**, 398 (1991).
- [5] J. Cook and K. W. Kemper, *Phys. Rev. C* **31**, 1745 (1985).
- [6] A. Etchegoyen, M. C. Etchegoyen, E. D. Izquierdo, D. Abriola, D. E. Di Gregorio, J. O. Fernández Niello, A. M. J. Ferrero, S. Gil, A. O. Macchiavelli, A. J. Pacheco, and J. E. Testoni, *Phys. Rev. C* **38**, 2124 (1988).
- [7] E. Steffens, W. Dreves, H. Ebinghaus, M. Köhne, F. Fiedler, P. Egelhof, G. Engelhardt, D. Kassen, R. Schäfer, W. Weiss, and D. Fick, *Nucl. Instrum. Methods* **143**, 409 (1977); D. Krämer, K. Becker, K. Blatt, R. Čaplar, D. Fick, H. Gemmeke, W. Haeberli, H. Jänsch, O. Karban, I. Koenig, L. Luh, K. -H. Möbius, V. Nečas, W. Ott, M. Tanaka, G. Tungate, I. M. Turkiewicz, A. Weller, and E. Steffens, *ibid.* **220**, 123 (1984).
- [8] A. J. Mendez, E. G. Meyers, K. W. Kemper, P. L. Kerr, E. L. Reber, and B. G. Schmidt, *Nucl. Instrum. Methods* (to be published).
- [9] H. G. Bingham, K. W. Kemper, and N. R. Fletcher, *Nucl. Phys.* **A175**, 374 (1971).
- [10] P. Egelhof, J. Barrette, P. Braun-Munzinger, W. Dreves, C. K. Gelbke, D. Kassen, E. Steffens, W. Weiss, and D. Fick, *Phys. Lett.* **84B**, 176 (1979).
- [11] *Polarization Phenomena in Nuclear Reactions*, edited by H. H. Barschall and W. Haeberli (University of Wisconsin Press, Madison, 1971).
- [12] P. D. Kunz (unpublished); J. R. Comfort (unpublished).
- [13] N. M. Clarke (unpublished).
- [14] J. Cook, K. W. Kemper, P. V. Drumm, L. K. Fifield, M. A. C. Hotchkis, T. R. Ophel, and C. L. Woods, *Phys. Rev. C* **30**, 1538 (1984).
- [15] H. Nishioka, R. C. Johnson, J. A. Tostevin, and K. -I. Kubo, *Phys. Rev. Lett.* **48**, 1795 (1982); H. Nishioka, J. A. Tostevin, R. C. Johnson, and K. -I. Kubo, *Nucl. Phys.* **A415**, 230 (1984); H. Ohnishi, M. Tanifuji, M. Kamimura, Y. Sakuragi, and M. Yahiro, *Nucl. Phys.* **A415**, 271 (1984); F. Petrovich, R. J. Philpott, A. W. Carpenter, and J. A. Carr, *Nucl. Phys.* **A425**, 609 (1984); S. P. Van Verst, D. P. Sanderson, D. E. Trcka, K. W. Kemper, V. Hnizdo, B. G. Schmidt, and K. R. Chapman, *Phys. Rev. C* **39**, 853 (1989); K. Rusek, J. Giroux, H. J. Jänsch, H. Vogt, K. Becker, K. Blatt, A. Gerlach, W. Korsch, H. Leucker, W. Luck, H. Reich, H. -G. Völk, and D. Fick, *Nucl. Phys.* **A503**, 223 (1989); Y. Hirabayashi and Y. Sakuragi, *ibid.* **A536**, 375 (1992).
- [16] B. A. Brown, A. Etchegoyan, N. S. Godwin, and W. D. M. Rae (unpublished).
- [17] C. N. Pinder, C. O. Blyth, N. M. Clarke, D. Barker, J. B. A. England, B. R. Fulton, O. Karban, M. C. Mannion, J. M. Nelson, C. A. Ogilvie, L. Zybert, R. Zybert, K. I. Pearce, P. J. Simmonds, and D. L. Watson, *Nucl. Phys.* **A533**, 25 (1991).
- [18] I. J. Thompson, University of Surrey 1991, version FRV (unpublished).
- [19] K. -I. Kubo, *Nucl. Phys.* **A246**, 246 (1975).